

Investigation of the foot-exposure impact in hyper-NA immersion lithography when using thin anti-reflective coating

Darron Jurajda^b, Enrico Tenaglia^a, Jonathan Jeauneau^b, Danilo De Simone^a, Zhimin Zhu^b,
Paolo Piazza^a, Paolo Piacentini^a, Paolo Canestrari^a

^aNumonyx S.r.l., R&D Technology Development, Via C. Olivetti 2, 20041 Agrate Brianza, Italy
^bBrewer Science, Inc., 2401 Brewer Drive, Rolla, Missouri 65401, USA

Key words: immersion, foot exposure (FE), effective reflectivity (ER), full diffraction model (FDM), bottom anti-reflective coating (BARC)

ABSTRACT

With immersion lithography at numerical aperture (NA) at or exceeding 1.2, the process window optimization of 42 nm line/space (L/S) patterning is a difficult challenge as the k_1 factor approaches 0.26, very close to the theoretical limit. Advanced immersion resists used to print these patterns are extremely thin and do not enable use of a thick bottom anti-reflective coating (BARC) due to etch selectivity limitations. Conventional BARC optimization based on reflectivity simulation alone does not provide an accurate process window as the resist profile is not fully correlated with substrate reflectivity. Reference experimental tests show that, by varying BARC thickness, we can obtain straighter profiles with 1.9% second-minimum reflectivity as compared to 0.3% first-minimum reflectivity. The Brewer Science, Inc., OptiStack™ simulation tool was used to simulate the optimal conditions based on a full diffraction model where the design criterion is the optical phase shift of the reflection. Two metrics comprise the simulation output: the foot exposure (FE) that characterizes the phase shift, and the effective reflectivity (ER) that is calculated from standing wave amplitude. The objective is to obtain the minimum ER at the target FE. Two experiments were conducted in order to validate this concept. In both set of tests, the films were characterized experimentally by analyzing the process window, resist profile, and line width roughness, and by simulating the FE and ER. In the first experiment a reference BARC, Brewer Science ARC®29A coating, and an advanced variable-k BARC, Brewer Science ARC®121 coating of the ARC®100 coating series, selected from simulation are compared. Even though the reference materials did not show a large variation of FE and ER in the wide thickness range studied, optical simulations explained the tapered profiles and the smaller process windows. The variable-k BARC presented a larger FE range that included both the target FE value and locally minimized ER. Process window analysis shows that the optimal process was not correlated to minimum reflectivity but to the metric previously described, minimum ER at target FE. The second experiment, designed to better de-correlate FE and ER through adapted k and thickness, using again an ARC®100 series BARC, confirmed the strong effect of FE value at a given ER on resist profiles and process window.

1. INTRODUCTION

As CDs are pushed smaller past 65 nm and resists become thinner, the importance of the ultraviolet (UV) distribution within the photoresist becomes greater. For resists with refractive indices of 1.6-1.7 the standing wave period is 55-60 nm and is approaching half the thickness of the photoresist in some cases. This means the location of constructive and destructive interference nodes resulting from any interface reflectivity can have a significant impact on the overall profile of the photoresist. At the same time, chemical interactions between BARCs and photoresists play an increasingly important role in profiles. This paper investigates the effects of the UV distribution on the photolithographic process using a new lithography metric, foot exposure (FE).^[1]

For a dedicated BARC chemistry, it is possible that the first and second minimum reflectivity points show different behaviors without any clear explanation until we introduce an additional parameter, FE, that seems have an effect on the bottom of the resist profile as shown in Figure 1.

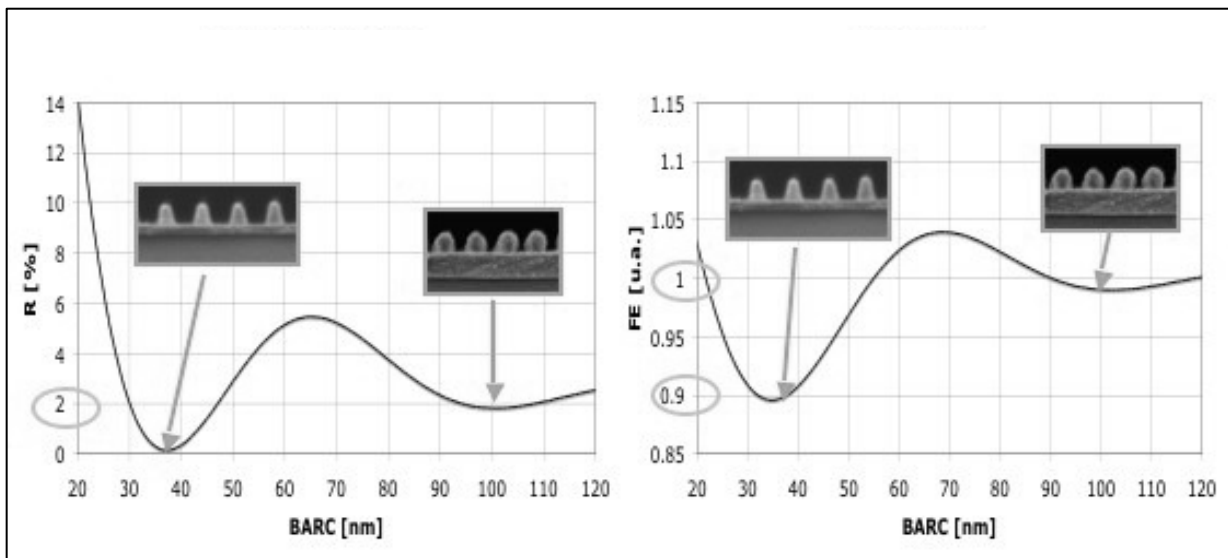


Figure 1. Example of reflectivity and FE simulation with associated cross sections on bare silicon

In order to understand the mechanism behind this phenomenon, we conducted two experiments to determine how best to utilize the FE metric. In the first experiment, litho results from two different BARCs are compared to their effective reflectivity (ER) and FE. The second experiment looks into the FE metric in more detail by choosing a BARC with a variable k value and then selecting different thickness and k values to produce a range of FE values while keeping ER constant. The ultimate goal is to determine what value the FE metric has in lithographic process development.

2. SIMULATION APPROACHES^[1]

Simulations were performed using Brewer Science, Inc., OptiStack™ simulation software. Conventional BARC simulation works in incident angles (or Fourier domain). It collects the reflectivity from all illumination and diffraction angles, and then gives a single value for overall reflectivity. One inconsistency that often arises is that the reflection from different diffraction angles is collected in an incoherent manner while lithography imaging is a coherent process. A second inconsistency is that, for incoherent illumination, the standing waves from different incident angles are shifted with respect to each other in the vertical direction, resulting in a smoothed standing wave. Thus, for a given overall reflectivity value, the standing wave amplitude depends also on the coherency of the illumination source, and it is unreasonable to set a reflectivity criterion for every possible optical setup. A third inconsistency is that a single reflectivity value does not contain the pattern-related details of the reflectivity. The reflectivity should be pattern dependent and distributed in the aerial image plane.

This simulation tool works on both Fourier and aerial image planes. For one illumination angle (or one illumination sigma point), the aerial image is obtained from the interference of forward and reflected images, and then the UV distribution is obtained from the accumulation of the images from all illumination angles. Finally, the resulting effective reflectivity is calculated from the standing wave amplitude of the UV distribution. In terms of standing wave control, the reflectivity criterion is independent of the optical setup. The distribution of the reflectivity in the aerial image plane depends on the mask pattern. Therefore pitch dependence can be analyzed within a mask. Effective reflectivity is evaluated in a photoacid diffusion region around line edges (25 nm to each side), ignoring the standing waves in an open area.

Foot exposure (FE) value is used to characterize the optical phase shift. In terms of chemical diffusion, UV intensity is taken into account only 50 nm around line edge and 40 nm from resist bottom. The UV distribution is weighed linearly from resist bottom as shown below in figure 2.

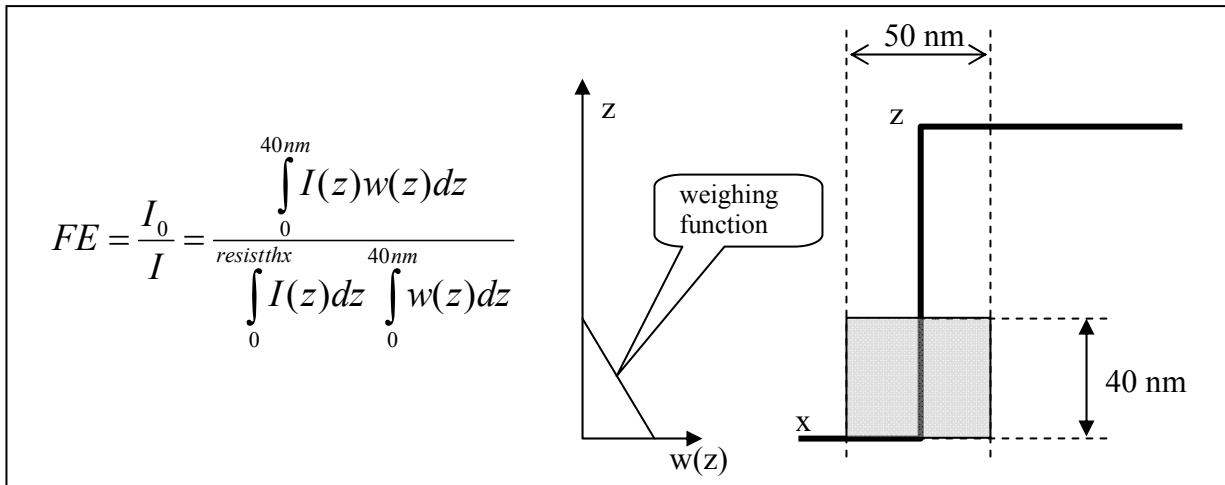


Figure 2. Foot exposure (FE) is the ratio of the intensity at the bottom of the resist line (I_0) to average intensity (I) through the full feature height. $w(z)$ represents the FE weight as function of the resist film thickness. In the run simulations we have considered the area between the first 40 nm of thickness in z direction and the portion of $\pm 25\text{nm}$ with respect to the edge of the resist line in x direction.

3. EXPERIMENTAL

Two experiments investigating FE were performed as outlined in tables 1 and 2. The first experiment utilized two different BARCs at different thicknesses to generate different combinations of effective reflectivity (ER) and foot exposure (FE). The second experiment utilized a variable k value BARC and adjusted the k value and thickness to give different FE values while keeping ER constant. A BARC that can be formulated with different k values was specifically chosen in order to minimize any chemical interaction effects.

BARC	n	k	Thickness (\AA)	ER (%)	FE
ARC [®] 29A	1.83	0.34	415	1.77	1.001
ARC [®] 29A	1.83	0.34	302	1.32	0.996
ARC [®] 29A	1.83	0.34	254	1.54	1.002
ARC [®] 29A	1.83	0.34	235	1.72	1.006
ARC [®] 121	1.67	0.21	530	0.13	0.955
ARC [®] 121	1.67	0.21	464	0.21	0.946
ARC [®] 121	1.67	0.21	363	1.22	0.953
ARC [®] 121	1.67	0.21	296	2.47	0.976
ARC [®] 121	1.67	0.21	244	3.63	1.001

Table 1. Experiment 1: BARC, n , k , thickness, ER and FE on bare wafers

BARC	n	k	Thickness (\AA)	ER (%)	FE
ARC [®] 129	1.67	0.28	508	0.35	0.911
ARC [®] 133	1.66	0.32	450	0.35	0.920
ARC [®] 133	1.66	0.32	537	0.35	0.954
ARC [®] 138	1.66	0.38	443	0.35	0.957

ARC [®] 138	1.66	0.38	483	0.35	0.968
ARC [®] 129	1.67	0.28	469	0.60	0.894
ARC [®] 129	1.67	0.28	545	0.60	0.933
ARC [®] 133	1.66	0.32	437	0.60	0.918
ARC [®] 133	1.66	0.32	555	0.60	0.963
ARC [®] 138	1.66	0.38	422	0.60	0.954
ARC [®] 138	1.66	0.38	508	0.60	0.977

Table 2. Experiment 2: BARC, n, k, thickness, ER and FE on bare wafers

For each process condition a focus exposure matrix was run to determine the process window (PW) with the selected resist (resist film thickness was equal to 900Å for all experiments mentioned in this paper). Process window analysis was performed using Brewer Science data software. Exposures were carried out on immersion ASML1700i linked to a Sokudo RF³ track. A Hitachi S9380I CDSEM was used for the CD measurements with target 42 nm ± 4 nm. Line width roughness was also carried out for L/S wafers using a dedicated CDSEM recipe for ArF resist. The optical and CDSEM settings are reported in table 3 and 4, respectively.

Tool	NA	Illumination
ASML1700i	1.2	Strong Dipole

Table 3. Optical settings

Tool	Accelerating Voltage	Probe Current	Magnification
CDSEM S-9380I	600 V	5.5 pA	150K → digital zoom 225Kx

Table 4. Hitachi CDSEM measurement settings

Finally, cross sections were analyzed using a Leo Ultra 55 tool at low energy with a dedicated recipe in order to avoid charging effects particularly strong when investigating ArF resists.

4. RESULTS

For each BARC thickness the process window was determined using critical dimension (CD) limits of 42 nm ± 4 nm and line width roughness (LWR) limits of < 5 nm. The process window area in this case is defined by the maximum and minimum CD in exposure and by the first occurrence of LWR greater than 5 nm in positive and negative focus as shown in Figure 3.

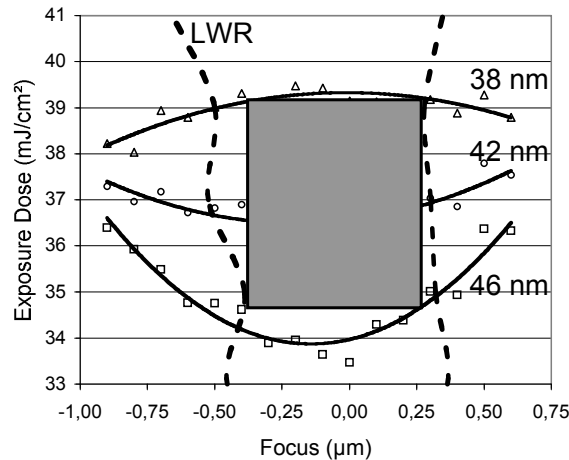


Figure 3. Process window area definition

As previously mentioned, the first experiment evaluated the performance of Brewer Science’s ARC®29A and ARC®121 coatings focusing on exposure latitude (EL) vs. depth of focus (DoF), process window and the associated cross sections for each thickness tested. In the second experiment, we used a variable k value BARC (ARC®129, ARC®133, ARC®138 coatings) in order to evaluate the relationship between the FE, process window size and the cross section profile at fixed reflectivity points less than 1%. From this data we were able to have some idea of the relative impact of the FE value.

4.1 ARC®29A coating

4.1.1 Simulations R and FE vs. ARC®29A coating thickness:

Thicknesses for ARC®29A coating near the first reflectivity minimum were chosen for this experiment. Effective reflectivity ranged from 1.32% to 1.77%. FE values ranged from 0.996 to 1.006 (Figure 4).

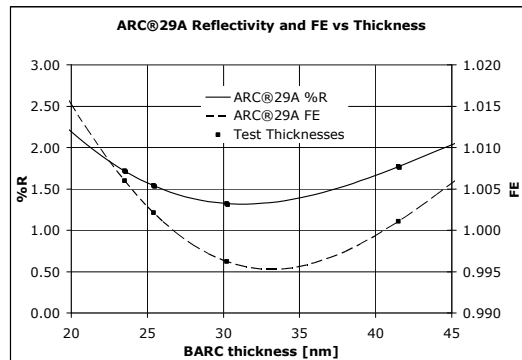


Figure 4. ARC®29A coating reflectivity and FE vs. thickness

4.1.2 EL vs. DoF and process window areas

The small FE and ER variation enabled by thickness variation do not show significant difference in process window performance (Figure 5).

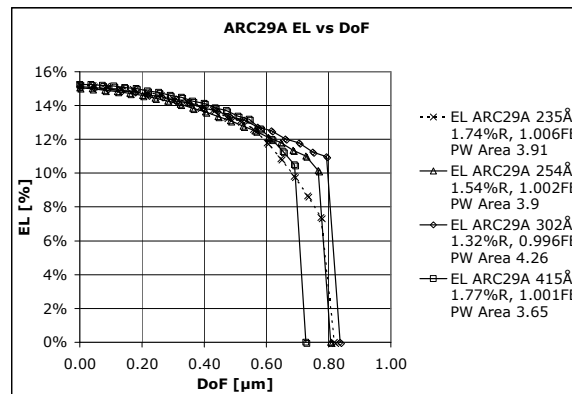


Figure 5. EL vs. DoF for ARC®29A coating

4.1.3 Cross sections:

Cross sections also confirm that FE and ER range of variation is not enough to cause resist profile variation (Table 5).

ARC@29A	415 Å	302 Å	254 Å	235 Å
R [%]	1.77	1.32	1.54	1.72
FE [u.a.]	1.001	0.996	1.002	1.006
Process Window Area	3.65	4.26	3.90	3.91

Table 5. ARC@29A coating cross sections with associated R, FE and process window areas

4.2 ARC@121:

4.2.1 Simulations R and FE vs. ARC@121 coating thickness:

Thicknesses for ARC@121 coating near the first reflectivity minimum were chosen for this experiment. Effective reflectivity ranged from 0.13% to 3.63%. FE values ranged from 0.946 to 1.001 (Figure 6).

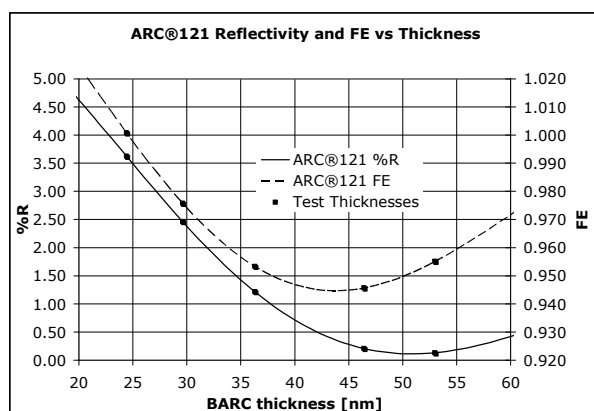


Figure 6. ARC@121 coating reflectivity and FE vs. thickness

4.2.2 EL vs DoF and process window areas

The large FE and ER variation accessible with ARC®121 coating has a visible impact on process performance (Figure 7 and Figure 8).

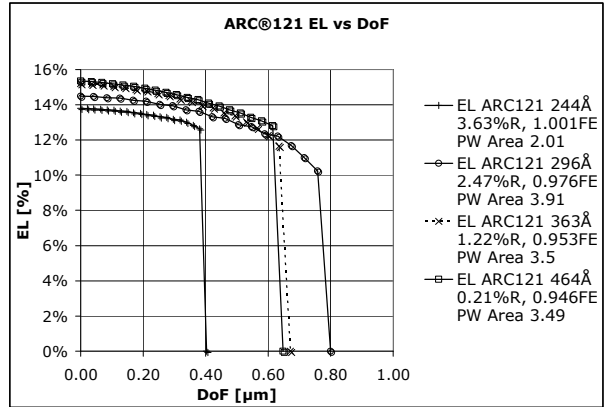


Figure 7. EL vs. DoF for ARC®121 coating

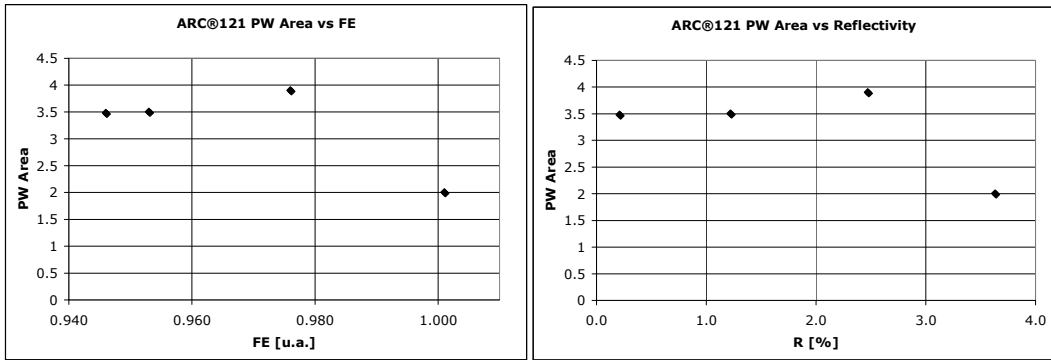


Figure 8. Process window area vs. FE and ER for ARC®121 coating

4.2.3 Cross sections

Cross sections confirm that resist profiles are strongly affected by the FE and ER. In fact, after the FE and ER range widening we are able to appreciate the resist profile modulation, but we are still unable to discriminate the contribution of the two parameters (Table 6).

ARC®121	530 Å	464 Å	363 Å	296 Å	244 Å
R [%]	0.13	0.21	1.22	2.47	3.63
FE [u.a.]	0.955	0.946	0.953	0.976	1.001
Process Window Area	N/A	3.49	3.50	3.91	2.01
	Slight Footing		Straight Profile		Undercutting

Table 6. ARC®121 coating cross sections with associated R, FE and process window areas

4.3 ARC@100 coating series (ARC@129, ARC@133 and ARC@138 coating)

From the first experiments it was difficult to separate the both FE and ER contribution on the process window and resist profile. In this second part of experiments we decided to work at a reflectivity less than 1% at the barc-photoresist interface and we modulated the FE metric keeping fixed the ER values.

In order to experimentally execute this work we made use of ARC@100 series where it is possible to tune the n and k values matching the requested reflectivity.

4.3.1 Simulations R and FE vs. ARC@100 coating series thickness

Three different k values and thicknesses near the first reflectivity minimum were chosen for this experiment. Points were selected to produce effective reflectivity values of 0.35% and 0.60%. For ER equal to 0.35%, FE values ranged from 0.911 to 0.968. For ER equal to 0.60%, FE values ranged from 0.894 to 0.977 (Figure 9).

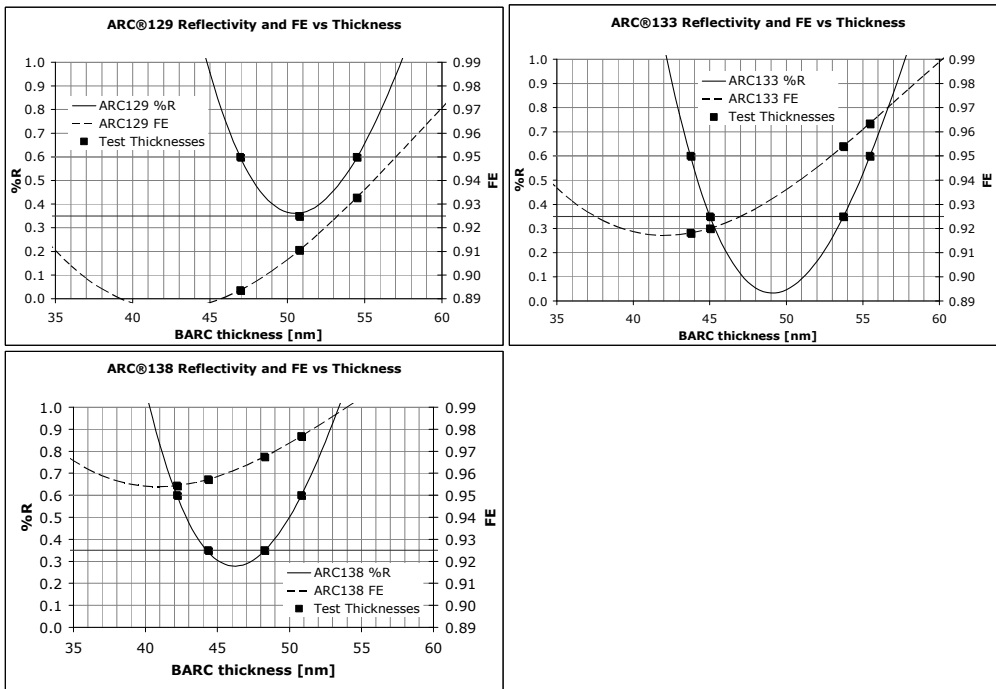


Figure 9. Reflectivity and FE vs. thickness for ARC@129, ARC@133 and ARC@138 coatings

4.3.2 EL vs. DoF and process window areas

Figure 10 shows process window variation (both exposure latitude and depth of focus) despite the constant ER.

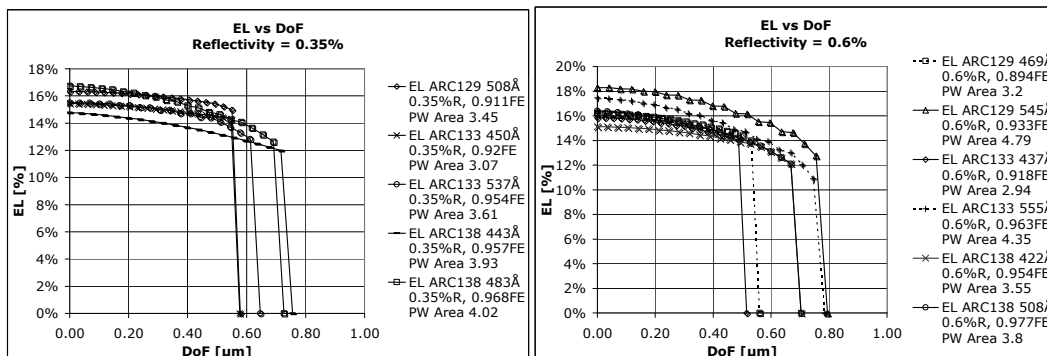


Figure 10. EL vs. DoF for ARC@100 coating series at 0.35% and 0.60% ER

Figure 11 shows that FE is the main driver for PW variations, in fact although the ER is kept the same (0.35% or 0.6% for each test) the PW increase by changing the FE metric (from 0.91 to 0.98).

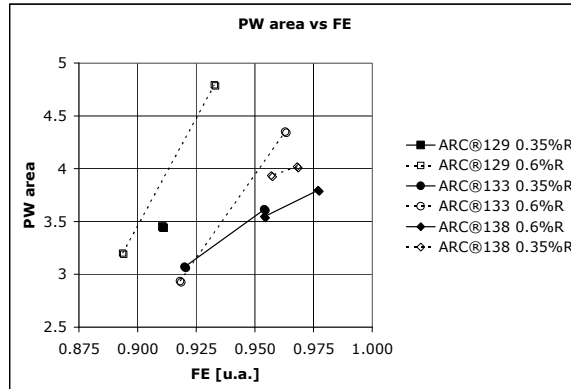


Figure 11. Process window area vs FE for ARC@100 Series

4.3.3 Cross sections of ARC@129 and ARC@138 coating (ER 0.35%, 0.6% at different FE)

Higher FE leads to straight profile and larger process window at a given ER (Table 6).

	ARC@129	ARC@138	ARC@129	ARC@138
Å	508	483	469	508
FE [u.a]	0.911	0.968	0.894	0.977
R [%]	0.35	0.35	0.60	0.60
LWR [nm]	4	3.6	3.8	3.7
CD 3σ [nm]	1.5	1.4	2	1.5
Process Window Area	3.45	4.02	3.20	3.8
	Footing	Straight Profile	Footing	Straight Profile

Table 6. ARC@100 coating series cross sections with associated R, FE, LWR, CD 3σ and process window areas

5. DISCUSSION

In general we have found the FE metric is difficult to separate from the reflectivity value without changing either the thickness of the BARC or the optical properties of the materials involved.

In the first experiment, the range of FE values (0.996 – 1.006) achievable near the first minimum of ARC®29A coating was too small to have any detectable impact on the process window or resist profiles. These FE values represent less than a 1% change in the amount of UV energy intensity at the bottom 40nm of the photoresist compared with the average intensity as determined by the definition of FE. The effective reflectivity (ER) varied from 1.32% - 1.74% and has the dominant impact on the process window size. The cross sections shown in Table 5 did not show a trend further suggesting the FE value range was too small. In order to understand whether the FE is an interesting parameter, a new BARC, ARC®121 coating, with a larger FE and ER range has been explored.

By using ARC®121 coating, we were able to explore a wider range of FE values (0.946 – 1.001) that represented a greater than 5% change in the amount of UV energy intensity in the bottom 40 nm of the photoresist. This was coupled with a range of ER from 0.13% - 3.63%. The process window size showed a strong drop with the highest ER value, but it was difficult to separate the contribution of the two parameters (Figure 8). Table 6 shows there is a relationship between ER value and photoresist profile, with values over 2% yielding an undercut profile and values less than 1% yielding a footing profile. In the end the best profile was an intermediate ER (1.22%) with FE close to 0.95, which suggests a complex matching phenomenon between ER and FE.

In the second experiment with reflectivity kept at fixed values we are able to see a clearer picture of the impact of FE on the process window and resist profiles. In this experiment the FE value ranges were 0.911 – 0.968 for ER equal to 0.35% and 0.894 – 0.977 for ER equal to 0.60%. As shown in Figure 12, within each material tested there is a trend of a larger process window as the FE value increases. Both ER values tested, 0.35% and 0.60%, have shown footing profiles when the FE value was near 0.9 [u.a.] and straight profiles when the FE value was near 0.97 [u.a.] as shown in Table 6. This data suggests there is a sensitive FE impact on the resist profile bottom when the reflectivity is less than 1%. It is theorized that as the footing profile increases, the LWR measurement increases in areas of defocus. This would explain the larger process window trend seen with larger FE values.

In this study, the impact of effective reflectivity (ER) and foot exposure (FE) simulation was deeply investigated. It was determined that the most desirable photoresist profile does not always correspond to a minimum of ER but rather a combination of ER and FE. The results have highlighted that the resist profile is tapered when the FE value is around 0.9 and straighter when close to 1.0 when ER is less than 1%. There is also a trend in larger process window as you move from FE 0.9 to FE 1.0 when ER is less than 1%. In conclusion, the FE metric has some value when pushing the limits of optical lithography and could potentially be used in the material selection process.

6. ACKNOWLEDGEMENTS

The authors would like to thank the Brewer Science R&D group and their continuous assistance in material synthesis and support, Kevin Schwalje from the Brewer Science Process Engineering Group for manufacturing the ARC®100 coating series samples, and special thanks to team members in the R2 Physics Lab for cross section analysis.

7. REFERENCES

[1] Zhimin Zhu., et al, "Reflection control in hyper-NA immersion lithography," *Proceedings of SPIE*, vol. 6924, 2008, pp. 69244A-1 - 69244A-7.